

# IOWA STATE UNIVERSITY

## Digital Repository

---

Chemical and Biological Engineering Publications

Chemical and Biological Engineering

---

1-11-2018

## Effect of corn and soybean oil derived additives on polymer-modified HMA and WMA master curve construction and dynamic modulus performance

Joseph H. Podolsky

*Iowa State University*, [podolsky@iastate.edu](mailto:podolsky@iastate.edu)

R. Christopher Williams

*Iowa State University*, [rwilliam@iastate.edu](mailto:rwilliam@iastate.edu)

Eric W. Cochran

*Iowa State University*, [ecochran@iastate.edu](mailto:ecochran@iastate.edu)

Follow this and additional works at: [https://lib.dr.iastate.edu/cbe\\_pubs](https://lib.dr.iastate.edu/cbe_pubs)

 Part of the [Civil Engineering Commons](#), [Polymer Science Commons](#), [Structural Engineering Commons](#), and the [Transportation Engineering Commons](#)

The complete bibliographic information for this item can be found at [https://lib.dr.iastate.edu/cbe\\_pubs/332](https://lib.dr.iastate.edu/cbe_pubs/332). For information on how to cite this item, please visit <http://lib.dr.iastate.edu/howtocite.html>.

---

This Article is brought to you for free and open access by the Chemical and Biological Engineering at Iowa State University Digital Repository. It has been accepted for inclusion in Chemical and Biological Engineering Publications by an authorized administrator of Iowa State University Digital Repository. For more information, please contact [digirep@iastate.edu](mailto:digirep@iastate.edu).

---

# Effect of corn and soybean oil derived additives on polymer-modified HMA and WMA master curve construction and dynamic modulus performance

## Abstract

In previous work, Isosorbide Distillation Bottoms (IDB), and other isosorbide and soybean based materials with similar properties were shown to act as antistrips in a polymer modified warm mix asphalt (WMA) at a 0.75% dosage level both through visual observations and statistical analysis of Hamburg Wheel Tracking Device (HWTDD) test results. Because of this evidence, there is an interest in how specimens produced with isosorbide and soybean bio-derived chemical additives would perform in the dynamic modulus test, as this is the main input used in AASHTOWare Pavement ME in the prediction of rutting performance. The main objective of this research is to compare and contrast dynamic modulus performance of two isosorbide, two soybean bio-derived chemical additive mixtures against each other and controls compacted at both hot mix asphalt (HMA) and WMA compaction temperatures. Master curve modeling with a proposed new (PN) model based on the Yang and You model and Booij and Thoone model for phase angle ( $\delta$ ) master curve construction led to the conclusion that proper placement of coefficients makes it possible to maintain precision and accuracy in the determination of  $E^*$  master curves while co-determining  $\delta$  master curves. From the master curve results, it was observed that some of the corn and soybean bio-derived chemical additives may be affecting the viscous behavior at intermediate and high test temperatures. Results from statistical analysis were inconclusive, and thus it is felt that further work must be done comparing HMA and WMA produced specimens in the HWTDD test.

## Keywords

Soybean, Isosorbide, Hot mix asphalt, Warm mix asphalt, Dynamic modulus, Master curves

## Disciplines

Chemical Engineering | Civil Engineering | Polymer Science | Structural Engineering | Transportation Engineering

## Comments

This is a manuscript of the article Podolsky, Joseph H., and R. Christopher Williams. "Effect of Corn and Soybean Oil derived Additives on Polymer-modified HMA and WMA Master Curve Construction and Dynamic Modulus Performance." *International Journal of Pavement Research and Technology* (2018). DOI: [10.1016/j.ijprt.2018.01.002](https://doi.org/10.1016/j.ijprt.2018.01.002). Posted with permission.

## Creative Commons License



This work is licensed under a [Creative Commons Attribution-Noncommercial-No Derivative Works 4.0 License](https://creativecommons.org/licenses/by-nc-nd/4.0/).



# Effect of corn and soybean oil derived additives on polymer-modified HMA and WMA master curve construction and dynamic modulus performance

Joseph H. Podolsky<sup>a,\*</sup>, R. Christopher Williams<sup>b</sup>, Eric Cochran<sup>c</sup>

<sup>a</sup> Iowa State University, Department of Civil, Construction, and Environmental Engineering, 174 Town Engineering Building, Ames, IA 50011, USA

<sup>b</sup> Iowa State University, Department of Civil, Construction, and Environmental Engineering, 486 Town Engineering Building, Ames, IA 50011, USA

<sup>c</sup> Department of Chemical & Biological Engineering, 1035 Sweeney, Ames, IA 50011, USA

Received 3 July 2017; received in revised form 10 October 2017; accepted 6 January 2018

## Abstract

In previous work, Isosorbide Distillation Bottoms (IDB), and other isosorbide and soybean based materials with similar properties were shown to act as antistrips in a polymer modified warm mix asphalt (WMA) at a 0.75% dosage level both through visual observations and statistical analysis of Hamburg Wheel Tracking Device (HWT) test results. Because of this evidence, there is an interest in how specimens produced with isosorbide and soybean bio-derived chemical additives would perform in the dynamic modulus test, as this is the main input used in AASHTOWare Pavement ME in the prediction of rutting performance. The main objective of this research is to compare and contrast dynamic modulus performance of two isosorbide, two soybean bio-derived chemical additive mixtures against each other and controls compacted at both hot mix asphalt (HMA) and WMA compaction temperatures. Master curve modeling with a proposed new (PN) model based on the Yang and You model and Booi and Thoonen model for phase angle ( $\delta$ ) master curve construction led to the conclusion that proper placement of coefficients makes it possible to maintain precision and accuracy in the determination of  $E^*$  master curves while co-determining  $\delta$  master curves. From the master curve results, it was observed that some of the corn and soybean bio-derived chemical additives may be affecting the viscous behavior at intermediate and high test temperatures. Results from statistical analysis were inconclusive, and thus it is felt that further work must be done comparing HMA and WMA produced specimens in the HWT test.

© 2018 Chinese Society of Pavement Engineering. Production and hosting by Elsevier B.V. This is an open access article under the CC BY-NC-ND license (<http://creativecommons.org/licenses/by-nc-nd/4.0/>).

**Keywords:** Soybean; Isosorbide; Hot mix asphalt; Warm mix asphalt; Dynamic modulus; Master curves

## 1. Introduction

The Kyoto Protocol ratified by the European Union (EU) in the mid-1990s provided the impetus for warm mix asphalt (WMA) to be developed. The mission of the

Kyoto Protocol was the lowering of emissions, and one clear way the asphalt industry could do this was by reducing production temperatures in asphalt mix plants. Thus, WMA was born. In 2002, the National Asphalt Pavement Association (NAPA) facilitated the introduction of WMA in the United States. To explore more opportunities presented through WMA use, a joint meeting between NAPA, the Federal Highway Administration (FHWA), and the National Center for Asphalt Technology (NCAT) was held in 2003. In 2004, a live demonstration of WMA being constructed was shown at the “World of Asphalt Show and

\* Corresponding author.

E-mail addresses: [podolsky@iastate.edu](mailto:podolsky@iastate.edu) (J.H. Podolsky), [rwilliam@iastate.edu](mailto:rwilliam@iastate.edu) (R.C. Williams), [ecochran@iastate.edu](mailto:ecochran@iastate.edu) (E. Cochran).

Peer review under responsibility of Chinese Society of Pavement Engineering.

Conference”. Three years later the FHWA’s International Technology Scanning Program sent a team of U.S. experts to visit Europe and evaluate the feasibility of WMA use in the United States. After touring four European countries with experience in WMA use they recommended WMA as an option for use in the United States as an alternative to HMA [1,2].

WMA is asphalt concrete that is mixed and compacted at temperatures 20–55 °C lower than those used to produce HMA. Due to temperature reductions, fuel usage and costs are decreased and emissions are lowered, and reduce worker exposure to fumes [1,3,4]. An additional benefit is the ability by contractors to extend the paving season in locations with colder climates and increase haul distances between production plants and laydown operations. To produce WMA, a variety of technologies are used including foaming, chemical, and organic/bio-derived [4–7].

WMA technologies are split into four subcategories: (1) foaming – water based, (2) foaming – water bearing additive, (3) chemical additive, and (4) organic/bio-derived additive. Water based foaming technologies such as the WAM-foam method, and the Double Barrel Green method introduce water to asphalt concrete to create a foaming effect, allowing lower production temperatures [8–10]. Water bearing additive technologies create a foaming effect in asphalt by releasing water during the mixing process of the additives with asphalt mix [8,11,12]. Chemical and organic/bio-derived additives reduce binder viscosity when they are blended with asphalt binder [13–16].

Isosorbide is a bio-derived product from corn with surfactant properties. A co-product during the production of Isosorbide, Isosorbide Distillation Bottoms (IDB) have also been shown to have surfactant-like properties [17]. As part of an earlier study it was found that IDB can be used as a WMA additive [18]. Additional research with the isosorbide and soybean based materials with similar properties to IDB were shown to improve the resistance against rutting and stripping of polymer modified WMA when used at a dosage level of 0.75% by weight of the binder [19]. Due to this observation, there is interest in how specimens produced with isosorbide and soybean bio-derived chemical additives would perform in the dynamic modulus test. There have been several past studies on dynamic modulus performance of WMA. Most have shown that WMA is more susceptible to rutting, and less prone to fatigue related distresses [20–25].

## 2. Objectives

The objectives of this research are to determine the effects from different isosorbide and soybean based additives on  $|E^*|$  and  $\delta$  performance in lab produced WMA through comparisons of master curves and statistical analysis.

## 3. Materials & methods

### 3.1. Material description

The experimental WMA additives included in this work are corn-derived isosorbide reactor product (RP), crude isosorbide (CI), soybean based epoxidized methyl soyate (EMS), and epoxidized soybean oil (ESO). The additives RP and CI were developed during the isosorbide-production process, while EMS was derived from ESO. RP, CI, EMS, and ESO are water-free material additives. Unlike CI and RP, EMS and ESO act as plasticizers in asphalt. The binder used is a polymer modified PG 64-28 that was pre-blended by a binder supplier located in North-west Iowa by blending 1.5% styrene-butadienestyrene (SBS) with a Montana crude PG 58-28 to achieve a PG 64-28 binder. In a past research study the dosage rate was optimized according to Superpave performance grading standards using control binders, binders modified with 0.50%, and 1% of an additive, IDB, with similar properties to the additives used in this work. In past research the optimum dosage level of IDB was found to be between 0.5% and 1.0% by weight of the binder in base binders from the same supplier because of the mass loss limit [18]. In this work, 0.75% was chosen as the upper limit dosage rate because past research showed that a 1% dosage level could not meet mass loss criteria [18]. More research with similar and the same additives when used at 0.75% showed that the binder grades do not change at low and high temperature [19,26]. Other WMA studies with chemical WMA additives have shown that the optimal dosage rate is approximately 0.5% by weight of binder [27]. To do equivalent comparisons and perform a valid statistical analysis, a dosage rate of 0.75% by weight of the binder for EMS, ESO, CI and RP was used. Each bio-additive was blended with the polymer-modified PG 64–28 binder using a Silverson shear mill at 140 °C  $\pm$  2 °C with a blending speed of 3000 rpm for one hour.

### 3.2. Preparation of asphalt mixtures

The mix design used to produce specimens was an approved 10 million ESAL design level surface mix from the Iowa Department of Transportation (DOT) and followed the design methods put down in Standard Specification Section 2303 from the Iowa DOT and Superpave Mix Design from AASHTO M323-13. Each specimen was compacted to a set height of 150 mm with a diameter of 100 mm to achieve  $7\% \pm 0.5\%$  air voids. All mixed specimens, with and without additives, were mixed at 140 °C. For HMA and WMA compaction, asphalt compaction temperatures of 140 °C and 120 °C were used. Each individual aggregate’s gradation, source information for each aggregate and the blend aggregate gradation are shown in Table 1. Individual aggregate gradations and the blend aggregate gradation was verified in the laboratory for the Iowa DOT job mix formula before specimens were

Table 1  
Mix design gradation and supplier information.

Source		Martin Marietta (Ames)	Martin Marietta (Ames)	Oldcastle Materials Group (Johnston)	Hallet (Ames)	Martin Marietta (Ames)	Martin Marietta (Ames)	Blend
Aggregate		12.5 mm Limestone	9.5 mm Limestone	Quartzite	Natural Sand	Manuf. Sand	Agg Lime	
U.S. Sieve	Sieve, mm	29% % Passing	16% % Passing	15% % Passing	13% % Passing	15% % Passing	12% % Passing	100% % Passing
3/4"	19.0	100.0	100.0	100.0	100.0	100.0	100.0	100.0
1/2"	12.5	79.7	100.0	100.0	100.0	100.0	100.0	94.1
3/8"	9.5	65.8	90.1	71.5	100.0	100.0	100.0	84.2
#4	4.75	37.2	20.5	5.1	96.8	95.2	99	53.6
#8	2.36	18.1	2.1	2.2	64.2	65.5	97	35.7
#16	1.18	12.5	0.7	2.0	33.7	36.3	75	22.9
#30	0.60	9.5	0.4	1.9	11.4	17.4	53	13.6
#50	0.30	7.5	0.3	1.9	0.9	6.5	38	8.2
#100	0.15	6.2	0.3	1.5	0.1	1.9	29	5.8
#200	0.075	5.2	0.3	1.2	0.0	0.8	22.3	4.5

produced for testing. Three specimens were constructed for each of the ten groups examined within this work (30 total specimens), and met the air void requirement of  $7\% \pm 0.5\%$  used for subsequent testing.

### 3.3. Dynamic modulus test

The dynamic modulus test is a linear viscoelastic test used to estimate the complex dynamic modulus  $|E^*|$  of asphalt mix specimens through each specimen's stress-strain relationship at several frequencies across multiple test temperatures. The complex dynamic modulus  $|E^*|$  is very important in that it is used to represent a pavement's stiffness from high to low temperatures and low to high frequencies under repeated traffic loading [28]. It is also variable with changing temperature and load frequency. This means comparing results across different test temperatures is very difficult. To make meaningful comparisons possible, master curves are developed. Master curves provide a means to achieve a visual representation of the results gained from testing at multiple test temperatures and frequencies [29]. For testing mix specimens in this research, three test temperatures (4.4, 21.1, and 37.8 °C) and nine frequencies ranging between 25 Hz and 0.1 Hz were used instead of five test temperatures and six frequencies. This is because research done by Li and Williams [30], found that three test temperatures (4.4, 21.1, and 37.8 °C) and nine frequencies rather than five test temperatures and six frequencies could produce the same final shape of the master curve and take less time to conduct the tests.

### 3.4. $|E^*|$ and $\delta$ master curves

For this research work all  $|E^*|$  master curves will be constructed using the sigmoidal function put forward by Pellinen and Witczak in 2002 [31]. There are however several ways to develop  $\delta$  master curves, where each approach

affects the shift and shape factors differently in the sigmoidal function. For this work, the benchmark phase angle master curve will be based on the model developed by Booij and Thoone [32] with a comparison made against a modified form of Booij and Thoone's model made by Yang and You [33]. In addition, another modification to Booij and Thoone's model on top of the modification made by Yang and You is proposed in this work to make predictions for both  $|E^*|$  master curves and phase angle master curves more accurate.

The sigmoidal function developed by Pellinen and Witczak [31] for constructing  $|E^*|$  master curves is shown below:

$$\log(|E^*|) = \delta + \frac{\alpha}{1 + e^{\beta + \gamma \log(1/f_r)}} \quad (1)$$

where  $|E^*|$  = dynamic modulus,  $f_r$  = reduced frequency at the reference test temperature,  $\delta$  = minimum modulus value,  $\delta + \alpha$  = maximum modulus value, and  $\beta, \gamma$  = parameters describing the shape of the sigmoidal function. The sigmoidal model shape parameters ( $\delta, \alpha, \beta$ , and  $\gamma$ ) are determined from back-calculation through the minimization of the sum of log squared error between estimated  $|E^*|$  values from the sigmoidal function to measured  $|E^*|$  values using the following equation.

$$Error^2 = \sum_{i=1}^n [\log(PredE_i^*) - \log(MeasE_i^*)]^2 \quad (2)$$

The time-temperature superposition (TTS) principle is used in the construction of master curves. The TTS principle addresses how data are shifted horizontally in either directions due to the fact that  $|E^*|$  values at low frequencies can be equal to  $|E^*|$  values gained from testing at higher temperatures. This is also true for  $|E^*|$  values at high frequencies and low-test temperatures. This makes it possible to shift  $|E^*|$  values from different test temperatures and frequencies to a single reference temperature. Because there are more frequencies than test temperatures, transitioning



from frequency to temperature is easier. To accomplish this transition a shift factor,  $a(T)$ , is determined for each test temperature using the following two equations:

$$f_r = \frac{f}{a(T)} \rightarrow \log(f_r) = \log(f) - \log(a(T)) \quad (3)$$

$$\log(a(T)) = a_1 T^2 + a_2 T + a_3 \quad (4)$$

where  $f_r$  = reduced frequency (loading frequency at reference temperature),  $f$  = loading frequency,  $a(T)$  = shift factor, and  $a_1$ ,  $a_2$ , and  $a_3$  are coefficients for solving the shift factor  $a(T)$ .

The first model relating  $|E^*|$  to  $\delta$  was developed in 1982 by Booij and Thoone, and was based on the Kramers–Konig relationship. Their model (known in this work as the BTS model) is shown in Eq. (5), where  $\delta(\omega)$  is the phase angle in radians/sec, and  $|E^*(\omega)|$  is the complex dynamic modulus. To convert angular frequency ( $\omega$ ) to reduced frequency Eq. (6) is used.

$$\delta(\omega) \approx \frac{\pi}{2} \frac{d \log(|E^*(\omega)|)}{d \log(\omega)} \quad (5)$$

$$f_r = \frac{\omega}{2\pi} \quad (6)$$

Substituting Eq. (6) into Eq. (1), and then substituting Eq. (1) into Eq. (5) gives the final expression of Booij and Thoone's model in Eq. (7):

$$\delta(f_r) \approx \frac{\pi}{2} \frac{\alpha \gamma}{(1 + e^{\beta - \gamma \log f_r})^2} e^{(\beta - \gamma \log f_r)} \quad (7)$$

where  $\delta(f_r)$  = phase angle in radians,  $f_r$  = reduced frequency in Hz, and  $\alpha$ ,  $\beta$ , and  $\gamma$  = shape parameters from Eq. (1). In 2015, Yang and You proposed a modification through the addition of another coefficient,  $c$  to Eq. (7), to make  $|E^*|$  and  $\delta$  predictions more accurate as shown in Eq. (8).

$$\delta(f_r) \approx c \frac{\pi}{2} \frac{\alpha \gamma}{(1 + e^{\beta - \gamma \log f_r})^2} e^{(\beta - \gamma \log f_r)} \quad (8)$$

In this work it is proposed that additional changes can be made to Yang and You's model to improve the accuracy of both  $|E^*|$  and  $\delta$  predictions, thus a change was made to the power expression, and the power 2 from Eqs. (7) and (8) was changed to  $x$ . The new model's expression is shown in Eq. (9).

$$\delta(f_r) \approx c \frac{\pi}{2} \frac{\alpha \gamma}{(1 + e^{\beta - \gamma \log f_r})^x} e^{(\beta - \gamma \log f_r)} \quad (9)$$

Shape parameters ( $\delta$ ,  $\alpha$ ,  $\beta$ , and  $\gamma$ ), shift factor coefficients ( $a_1$ ,  $a_2$ , and  $a_3$ ), and  $c$  and  $x$  are determined for Eqs. (1), (4), (7), (8) and (9) through the minimization of the sum of log squared error between predicted  $|E^*|$  and  $\delta$  values and the measured values using the following equation.

$$\begin{aligned} Error^2 = & \sum_{i=1}^n [\log(Pred E_i^*) - \log(Meas E_i^*)]^2 \\ & + \sum_{i=1}^n [\log(Pred \delta_i) - \log(Meas \delta_i)]^2 \end{aligned} \quad (10)$$

Table 2  
Summary of master curve fitting parameters for HMA and WMA using sigmoidal model.

Name		Control		EMS		ESO		CI		RP	
Compaction temperature (°C)		120	140	120	140	120	140	120	140	120	140
Shape factors	$\delta$	4.25	3.09	3.49	3.07	3.19	3.65	3.00	2.53	3.12	3.02
	$\alpha$	2.13	3.44	2.95	3.46	3.32	2.85	3.55	4.08	3.37	3.53
	$\beta$	−0.25	−0.93	−0.67	−0.90	−0.73	−0.68	−0.88	−1.16	−0.89	−0.99
	$\gamma$	0.73	0.51	0.58	0.52	0.54	0.54	0.47	0.45	0.54	0.51
Shift factors	$a_1$	3.87E−04	4.68E−04	6.49E−04	2.94E−04	8.24E−04	5.41E−04	1.72E−04	1.64E−04	4.06E−04	3.23E−04
	$a_2$	−0.13	−0.13	−0.14	−0.12	−0.14	−0.14	−0.12	−0.12	−0.13	−0.12
	$a_3$	2.48	2.48	2.68	2.43	2.63	2.63	2.40	2.47	2.49	2.45

Table 3  
Summary of master curve fitting parameters for HMA and WMA using BTS model.

Name		Control		EMS		ESO		CI		RP	
Compaction temperature (°C)		120	140	120	140	120	140	120	140	120	140
Shape factors	$\delta$	3.70	3.45	3.51	3.43	3.44	3.71	3.45	3.23	3.40	3.37
	$\alpha$	2.87	3.14	3.06	3.16	3.14	2.86	3.15	3.40	3.19	3.23
	$\beta$	−0.45	−0.70	−0.52	−0.67	−0.55	−0.57	−0.63	−0.87	−0.67	−0.79
	$\gamma$	0.50	0.48	0.49	0.50	0.51	0.49	0.47	0.46	0.49	0.49
Shift factors	$a_1$	4.71E−04	2.50E−04	3.56E−04	5.77E−05	6.22E−04	3.86E−04	−6.32E−05	−5.97E−05	1.40E−04	1.22E−04
	$a_2$	−0.13	−0.12	−0.13	−0.12	−0.14	−0.13	−0.11	−0.12	−0.12	−0.12
	$a_3$	2.62	2.49	2.67	2.43	2.65	2.62	2.38	2.45	2.51	2.45

Table 4

Summary of master curve fitting parameters for HMA and WMA using YY model.

Name	Control		EMS		ESO		CI		RP		
Compaction temperature (°C)	120	140	120	140	120	140	120	140	120	140	
Shape factors	$\delta$	3.71	3.36	3.45	3.36	3.37	3.68	3.40	3.17	3.30	3.31
	$\alpha$	2.86	3.26	3.16	3.27	3.25	2.90	3.23	3.48	3.33	3.31
	$\beta$	−0.44	−0.70	−0.52	−0.67	−0.55	−0.57	−0.62	−0.87	−0.67	−0.78
	$\gamma$	0.50	0.50	0.50	0.51	0.52	0.50	0.48	0.47	0.51	0.50
	$c$	1.00	0.91	0.91	0.91	0.91	0.96	0.93	0.93	0.89	0.93
Shift factors	$a_1$	4.65E−04	2.15E−04	3.21E−04	3.38E−05	5.67E−04	3.57E−04	−7.83E−05	−7.22E−05	1.06E−04	9.96E−05
	$a_2$	−0.13	−0.12	−0.13	−0.11	−0.13	−0.13	−0.11	−0.11	−0.11	−0.11
	$a_3$	2.62	2.33	2.51	2.27	2.48	2.53	2.26	2.32	2.31	2.32

Table 5

Summary of master curve fitting parameters for HMA and WMA using PN model.

Name	Control		EMS		ESO		CI		RP		
Compaction temperature (°C)	120	140	120	140	120	140	120	140	120	140	
Shape factors	$\delta$	3.81	2.73	2.98	2.77	2.91	3.38	2.82	2.52	2.62	2.73
	$\alpha$	2.77	3.84	3.57	3.79	3.66	3.16	3.74	4.08	3.94	3.84
	$\beta$	−0.36	−1.03	−0.80	−0.98	−0.81	−0.76	−0.94	−1.18	−1.02	−1.07
	$\gamma$	0.51	0.47	0.48	0.48	0.49	0.48	0.45	0.45	0.48	0.48
	$c$	0.93	1.14	1.14	1.14	1.11	1.11	1.17	1.15	1.14	1.13
	$x$	1.88	2.62	2.50	2.58	2.46	2.32	2.56	2.60	2.66	2.54
Shift factors	$a_1$	3.51E−04	5.24E−04	6.41E−04	3.44E−04	8.53E−04	5.71E−04	2.31E−04	2.15E−04	4.49E−04	3.69E−04
	$a_2$	−0.13	−0.13	−0.14	−0.13	−0.15	−0.14	−0.12	−0.12	−0.13	−0.13
	$a_3$	2.55	2.54	2.72	2.48	2.68	2.67	2.46	2.52	2.54	2.51

### 3.5. Setup of ANOVA

For the statistical analysis of the measured  $|E^*|$  and  $\delta$  results two separate analyses of variances (ANOVA)s were conducted to examine how the factors: additive, compaction temperature, test temperature, and frequency,

and their interactions affect performance. A split plot repeated measured (SPRM) design was used for each analysis. The whole plots were additive (A) and compaction temperature (B), while the sub plot factors examined were test temperature (°C) – (C) and frequency (Hz) – (D) Randomization was done by randomizing the order in

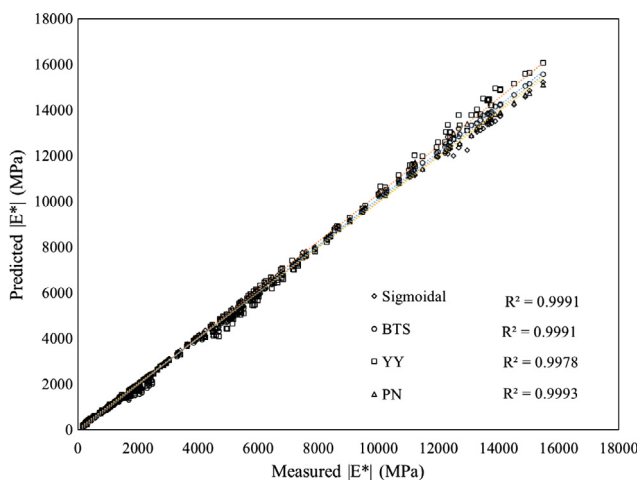


Fig. 1. Comparison of predicted against measured  $|E^*|$  results for the 10 asphalt mixtures (810 data points) for sigmoidal model, BTS model, YY Model, and PN model.

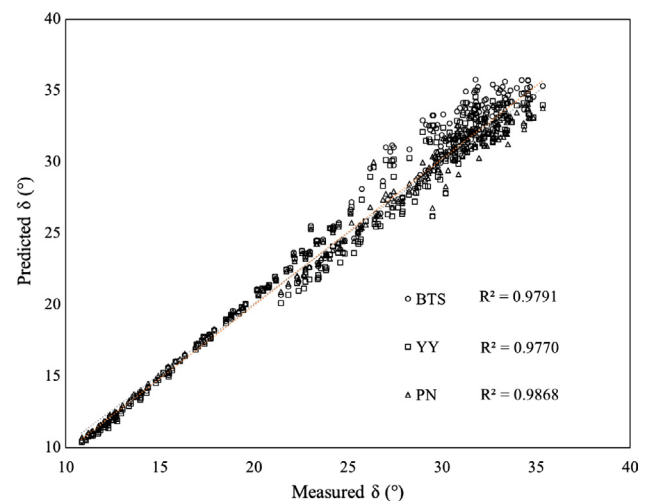


Fig. 2. Comparison of predicted against measured  $\delta$  results for the 10 asphalt mixtures (810 data points) for BTS model, YY model, and PN model.

which specimens from different groups and compaction temperatures were tested at each test temperature. The results of the statistical analysis are shown in Section 4.4.

## 4. Results & discussion

### 4.1. Master curve parameters & prediction data verification

A summary of all the shape and shift factors for the sigmoidal model, BTS model, YY model, and the proposed

Table 6  
Summary of information criteria results.

Model name	SSE	<i>n</i>	<i>p</i>	AIC <sub>p</sub>	BIC <sub>p</sub>	APC <sub>p</sub>
$ E^* $						
Sigmoidal	4197582.82	270	4	2613.931	2628.32	16014.17
BTS	4470651.2	270	4	2630.948	2645.34	17055.95
YY	11597712.8	270	5	2890.332	2908.32	44575.42
PN	3504798.04	270	6	2569.23	2590.82	13570.77
$\delta$						
BTS	328.488289	270	4	60.94	75.34	1.25
YY	331.285488	270	5	65.23	83.22	1.27
PN	174.246363	270	6	−106.25	−84.66	0.67

new (PN) model used for constructing  $|E^*|$  and  $\delta$  master curves are shown in Tables 2 through 5. For verification purposes comparisons between measured and predicted  $|E^*|$  and  $\delta$  data for all the mixtures were plotted in Figs. 1 and 2 for the aforementioned master curve fitting models, except the sigmoidal model for  $\delta$ . A total of 810 points were plotted for each model's fitted curve ( $|E^*|$  and  $\delta$ ). For verification of the  $|E^*|$  and  $\delta$  prediction models, comparisons were made between predicted results and measured results as shown in Figs. 1 and 2. Fig. 1 displays the  $|E^*|$  results for all 10 asphalt mixtures gained through the sigmoidal, Booij and Thoone (BTS), Yang and You (YY), and proposed new (PN) models.

In past research, the sigmoidal model has been shown to be highly accurate in the prediction of  $|E^*|$  [34,35]. In this research, the sigmoidal model was used as a benchmark to compare the accuracy of the other prediction models. Past researchers assumed that when a model takes into account the  $\delta$  as well as  $|E^*|$ , some of the optimization of  $|E^*|$  is sacrificed [33]. For the YY model, the coefficient of determination ( $R^2$ ) is slightly lower than the  $R^2$  from the sigmoidal model. However, this is not the case for the BTS model and the PN model in this research as these models have  $R^2$  values either equal or greater than the  $R^2$

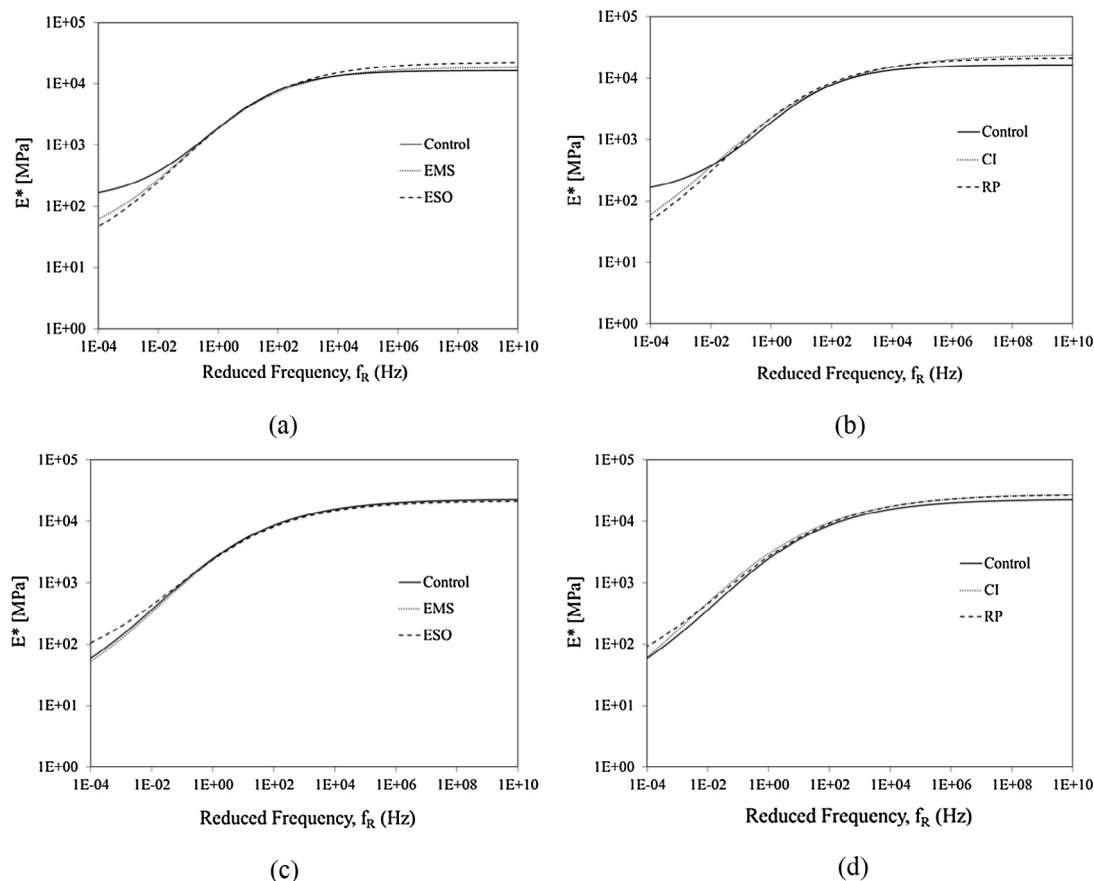


Fig. 3.  $|E^*|$  master curves of different additives against control using sigmoidal model, (a) soybean compacted at 120 °C, (b) corn compacted at 120 °C, (c) soybean compacted at 140 °C, and (d) corn compacted at 140 °C.



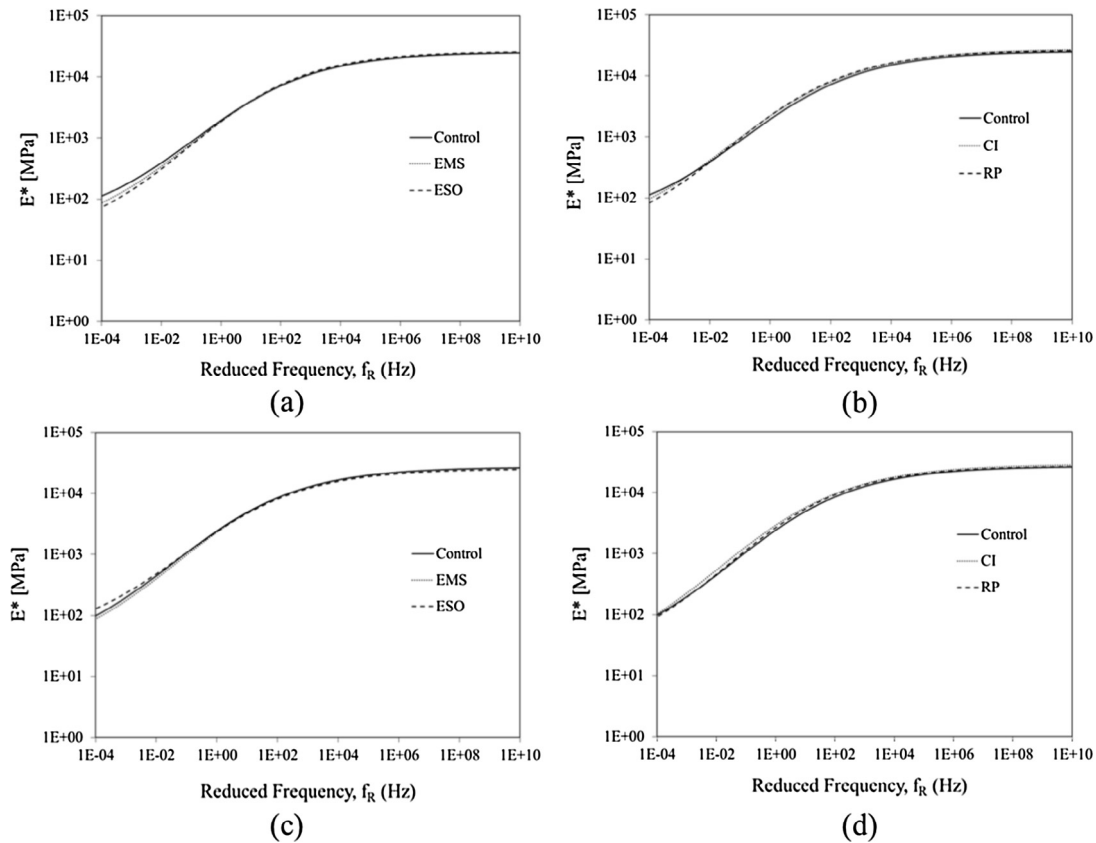


Fig. 4.  $|E^*|$  master curves of different additives against control using BTS model, (a) soybean compacted at 120 °C, (b) corn compacted at 120 °C, (c) soybean compacted at 140 °C, and (d) corn compacted at 140 °C.

value for the sigmoidal model. This contradicts past belief that use of  $\delta$  data causes sacrifice of the  $|E^*|$  optimization. To gain the same predictive quality or better could be more dependent on the testing regimen for gaining data as well as the placement of new coefficients in models.

Fig. 2 displays the predicted  $\delta$  results gained from the BTS, YY, and PN models vs. the measured  $\delta$  results for the 10 asphalt mixtures. Historically, past research has shown that the YY model was more accurate than the BTS model in the determination of  $\delta$  master curves [33,36]. However, this is not the case for the measured data used in this work. The  $R^2$  for the YY model is lower than the  $R^2$  values determined for the BTS and PN model. The result of the BTS model's  $R^2$  value contradicts the past assertion that just by adding another coefficient, the model will become more accurate. The number of coefficients added is not important, but rather the placement of the coefficients within the model's equation is more important in terms of model accuracy. This is shown by the  $R^2$  for the PN model being higher than the YY model, as the PN model is a modified version of the YY model with the substitution of a coefficient for 2nd power on the bottom of Eq. (8), which then turns into Eq. (9). Not only is there no sacrifice in  $|E^*|$  optimization due to optimization for the  $\delta$  master curve, but both  $|E^*|$  and  $\delta$  master curves outperform the sigmoidal model, and the other two models. Thus, place-

ment of new coefficients is the most important step in optimizing these type of models.

Three information criteria were used for comparing the models to one another to select three out of the four for further analysis. They were Akaike Information Criterion (AIC), Bayesian Information Criterion (BIC) and Amemiya's Prediction Criterion (APC). These criteria combine information such as the sum of square error (SSE), number of model parameters ( $p$ ), and the sample size ( $n$ ) of each model to come up with an information criterion value. The lower the value the better the model is. The following three equations, Eq. (11) (AIC), Eq. (12) (BIC), and Eq. (13) (APC) are shown below:

$$\text{AIC} = n \ln(\text{SSE}) - n \ln(n) + 2p \quad (11)$$

$$\text{BIC} = n \ln(\text{SSE}) - n \ln(n) + p \ln(n) \quad (12)$$

$$\text{APC} = \frac{(n+p)}{n(n-p)} \text{SSE} \quad (13)$$

Due to both  $|E^*|$  and  $\delta$  models being solved simultaneously for the BTS, YY and PN models, the  $p$  values were kept the same for each model's determination of each information criteria. As shown from the results in Table 6, the lowest value from the three criteria was held by PN model for both  $|E^*|$  and  $\delta$  models. The second lowest value was held by the sigmoidal model for  $|E^*|$  and the BTS model for  $\delta$ . The model with the least accurate predicting

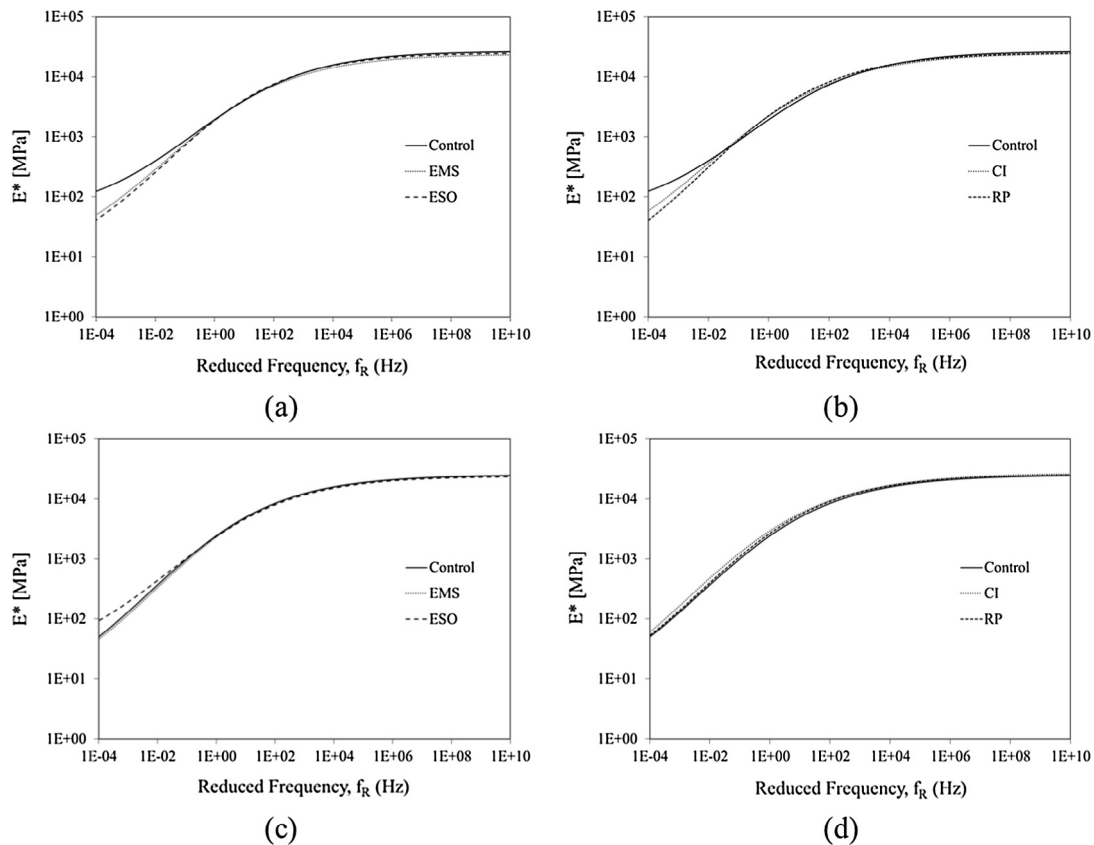


Fig. 5.  $|E^*|$  master curves of different additives against control using PN model, (a) soybean compacted at 120 °C, (b) corn compacted at 120 °C, (c) soybean compacted at 140 °C, and (d) corn compacted at 140 °C.

ability was the YY model for  $|E^*|$  and  $\delta$  models. After examining these analysis results the three models selected for further analysis and discussion were the Sigmoidal, BTS, and PN models.

#### 4.2. $|E^*|$ master curves

Using the master curve fitting parameters shown in Tables 2, 3 and 5, master curve plots were created for all mixture groups in Figs. 3, 4, and 5. From the results, at low temperatures/high reduced frequencies there are no visual differences between the three groups shown in each sub plot. However, at high temperatures/low reduced frequencies, there are visual differences between groups within each compaction temperature (WMA and HMA), and there are differences between compaction temperatures for the same group. This situation is clearly shown in Fig. 3(a–d). It is also displayed in Figs. 4 and 5. The results display that the corn and soybean based additives soften the dynamic modulus at high temperatures for WMA against the control WMA, whereas for HMA they stiffen the dynamic modulus against the control HMA. This occurs in the results from the sigmoidal, BTS, and PN models.

As dynamic modulus test results are used as performance input parameters in AASHTOWare Pavement

ME, these results can be used to predict pavement performance, e.g. rutting and fatigue cracking. For further analysis beyond visual observations, statistical analysis must be done as shown in Section 4.4.

#### 4.3. $\delta$ Master curve results

From the  $\delta$  master curve fitting parameters in Tables 3 and 5,  $\delta$  master curve plots were constructed as shown in Figs. 6 and 7. The results in Fig. 6 illustrate that the corn and soybean based additives make asphalt mix more viscous at intermediate and high temperatures for both HMA and WMA when compared against the results of the control groups. This is not the case for the ESO modified HMA as it is more elastic at intermediate and high temperatures than the control HMA. At low temperature, the  $\delta$  master curves for all groups overlap, and thus no visual differences can be observed. More differences were observed between groups within compaction temperatures and for compaction temperatures within the same group in Fig. 7 for the PN model than for the BTS model's results in Fig. 6. At WMA mixing and compaction temperatures, the corn and soybean modified asphalt mixtures appear to be more elastic at high temperatures, while at intermediate temperatures slightly to more viscous than the control WMA. This is not shown at HMA mix and compaction

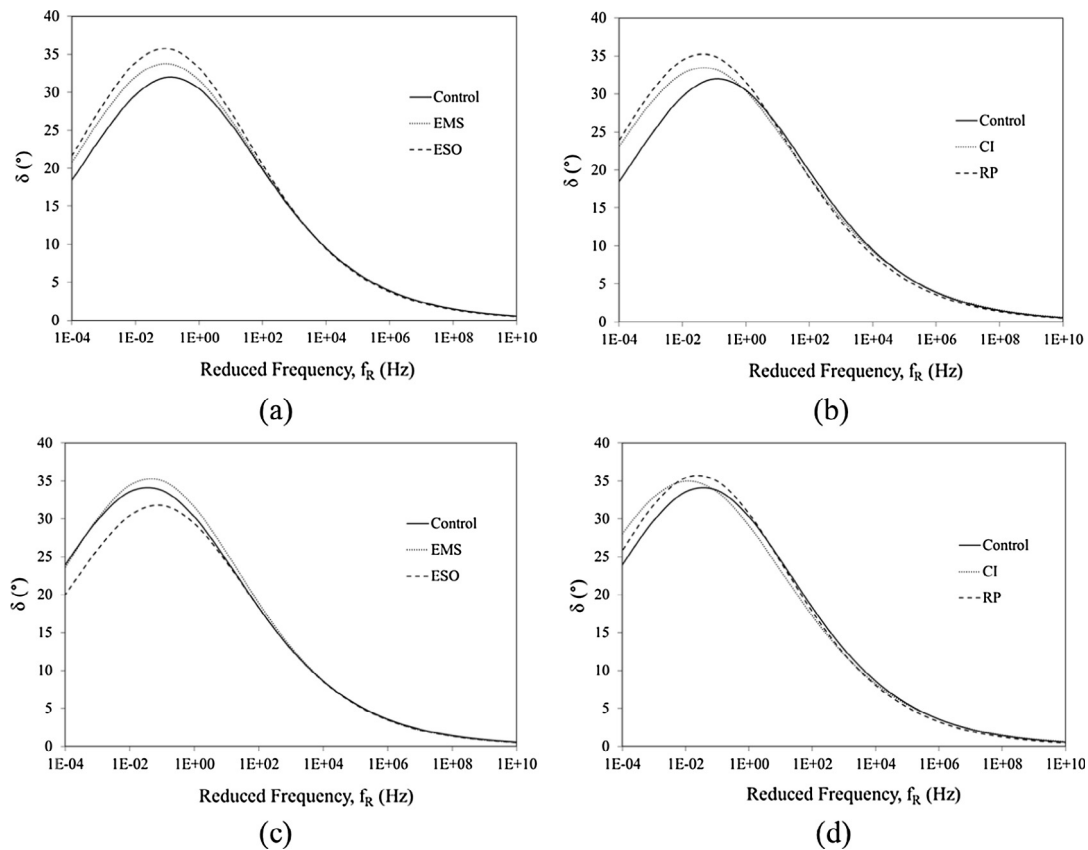


Fig. 6.  $\delta$  master curves of different additives against control using BTS model, (a) soybean compacted at 120 °C, (b) corn compacted at 120 °C, (c) soybean compacted at 140 °C, and (d) corn compacted at 140 °C.

temperatures. For the soybean-based materials, EMS makes the mix more viscous while the ESO makes the mix more elastic at intermediate temperatures compared to the control HMA. The corn-based materials make HMA more viscous at intermediate and high temperatures when compared to the control HMA. The visual results do not show clear trends, so no conclusions can be made in terms of if the bio-additives are affecting the viscous or elastic properties at high and intermediate temperatures. To better understand if these materials are making the mix more viscous or elastic, further work such as a statistical analysis was done as shown in Section 4.4.

#### 4.4. Statistical analysis of non-shifted data

The measured dynamic modulus values were gained from testing at test temperatures (4.4, 21.1, and 37.8 °C), each at multiple frequencies (0.1, 0.2, 0.5, 1, 2, 5, 10, 20, and 25 Hz) for three specimens from each group – 10 (total of 30 test specimens). All measured data (810 data points) were used in statistical analysis, as no outliers were found during testing, e.g. 95% of the measured data from each group fell within two standard deviations of each group's mean. All interactions between A, B, C, and D were examined. The two ANOVA analyses are shown in Tables 7 and 8. In both analyses, factors/interactions were significant at

a 95% level of confidence if the p-value is less or equal to 0.05. From Tables 7 and 8 the main factors and interactions of interest are A, B, A\*B, and A\*B\*C. For  $E^*$ , all except for the interaction of A\*B are significant sources of variability. For  $\delta$ , all except the factor A are significant sources of variability. This means that for  $E^*$ , overall there are no statistical differences between the groups across both compaction temperatures. However, when looking at all the groups for both compaction temperatures against temperature there are significant differences. This result agrees with the findings shown in the  $E^*$  master curve plots, that with different compaction temperatures, the groups behave differently from low to high temperatures. For  $\delta$ , groups (A) were found to be not different from one another according to a 95% confidence level, but interactions of A with other factors except frequency were significant sources of variability.

To examine the interaction between additive (A) and compaction temperature (B) for both  $E^*$  and  $\delta$ , the student's t-test was done to determine the least square mean differences as shown in Fig. 8. When the same letter does not connect levels, those levels are statistically significantly different at a 95% confidence limit. Even though the ANOVA analysis outcome was said that the interaction of A\*B was not significant for  $E^*$ , the results in Fig. 8(a) reach a different conclusion. For RP, CI, and EMS there

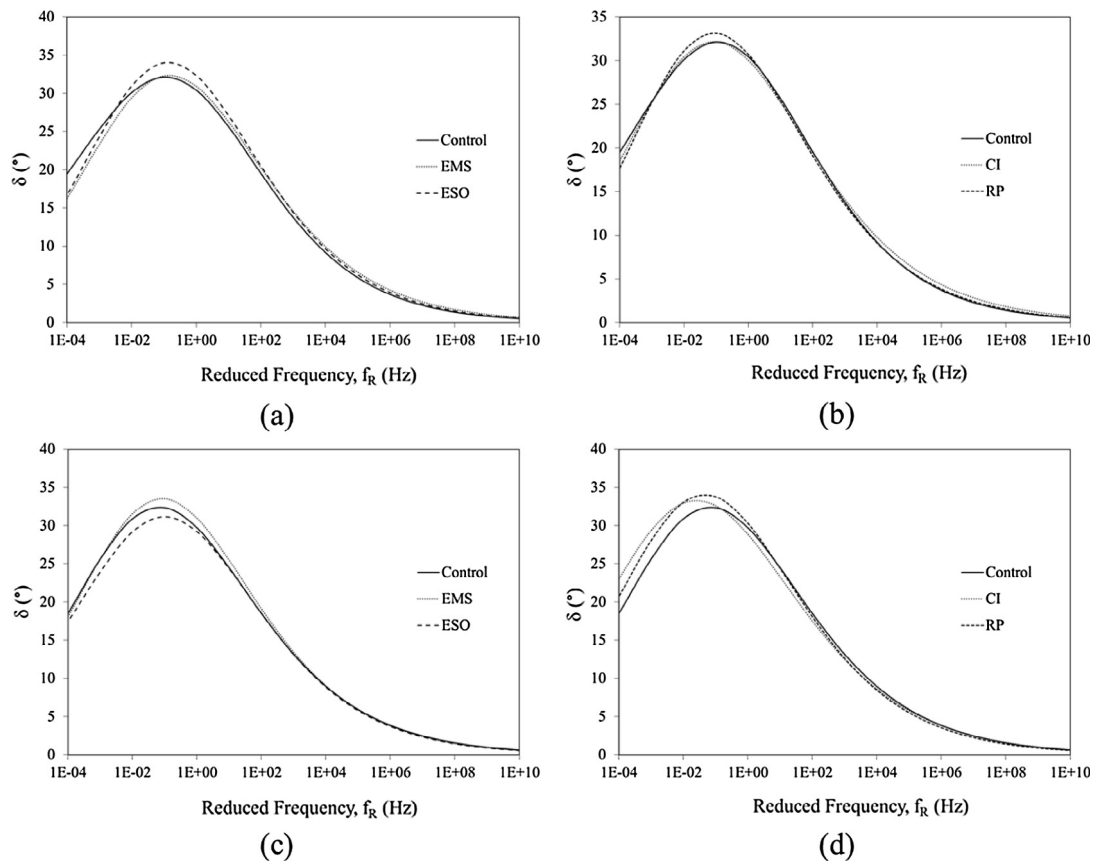


Fig. 7.  $\delta$  master curves of different additives against control using PN model, (a) soybean compacted at 120 °C, (b) corn compacted at 120 °C, (c) soybean compacted at 140 °C, and (d) corn compacted at 140 °C.

Table 7  
 $E^*$  ANOVA results.

Source	DF	SS	MS	F ratio	Prob > F	Significant
A	4	3.02E+07	7.56E+06	4.65	0.0082	Yes
B	1	7.05E+07	7.05E+07	43.33	<0.0001	Yes
C	2	1.09E+10	5.44E+09	78125.35	<0.0001	Yes
D	8	2.69E+09	3.36E+08	4830.87	<0.0001	Yes
A*B	4	1.10E+07	2.74E+06	1.68	0.193	No
A*C	8	1.19E+07	1.49E+06	21.44	<0.0001	Yes
A*D	32	3.45E+06	1.08E+05	1.55	0.0298	Yes
B*C	2	2.20E+07	1.10E+07	157.94	<0.0001	Yes
B*D	8	5.98E+06	7.48E+05	10.74	<0.0001	Yes
C*D	16	8.27E+08	5.17E+07	742.76	<0.0001	Yes
A*B*C	8	9.39E+06	1.17E+06	16.87	<0.0001	Yes
A*B*D	32	2.42E+06	7.56E+04	1.09	0.3447	No
A*C*D	64	6.79E+05	1.06E+04	0.15	1	No
B*C*D	16	2.68E+05	1.68E+04	0.24	0.9991	No
A*B*C*D	64	1.19E+06	1.85E+04	0.27	1	No
Specimen No. [A, B] & random	20	3.25E+07	1.63E+06	23.39	<0.0001	Yes

Note: A – Additive, B – Compaction Temperature, C – Test Temperature (°C), and D – Frequency (Hz).

Note: DF – degrees of freedom, SS – sum of squares, MS – mean square.

is a difference in performance based on compaction temperature. In addition, there is a difference between the HMA and WMA controls. Even though the results for  $\delta$  in Table 8 concludes there are statistical differences for the interaction between A\*B, there is only one clear visible

statistical difference, a difference between ESO produced at WMA compaction temperatures vs. ESO produced at HMA compaction temperatures. Thus, the  $\delta$  results do not meet the expectations as set from the ANOVA analysis results.

Table 8  
 $\delta$  ANOVA results.

Source	DF	SS	MS	F ratio	Prob > F	Significant
A	4	3.90E+01	9.74E+00	1.43	0.2596	No
B	1	7.53E+01	7.53E+01	11.08	0.0033	Yes
C	2	3.12E+04	1.56E+04	10554.10	<0.0001	Yes
D	8	3.31E+03	4.14E+02	279.71	<0.0001	Yes
A*B	4	1.93E+02	4.82E+01	7.10	0.001	Yes
A*C	8	1.23E+02	1.53E+01	10.36	<0.0001	Yes
A*D	32	4.41E+01	1.38E+00	0.93	0.5776	No
B*C	2	9.83E+01	4.92E+01	33.21	<0.0001	Yes
B*D	8	3.37E+01	4.21E+00	2.85	0.0042	Yes
C*D	16	4.90E+03	3.06E+02	206.99	<0.0001	Yes
A*B*C	8	8.86E+01	1.11E+01	7.49	<0.0001	Yes
A*B*D	32	3.90E+01	1.22E+00	0.82	0.745	No
A*C*D	64	7.80E+01	1.22E+00	0.82	0.8308	No
B*C*D	16	4.71E+01	2.94E+00	1.99	0.0124	Yes
A*B*C*D	64	5.63E+01	8.80E-01	0.59	0.9945	No
Specimen No. [A, B] & random	20	1.36E+02	6.80E+00	4.59	<0.0001	Yes

Note: A – Additive, B – Compaction Temperature, C – Test Temperature (°C), and D – Frequency (Hz).

Note: DF – degrees of freedom, SS – sum of squares, MS – mean square.

$\alpha = 0.050$ $t = 2.08596$			$\alpha = 0.050$ $t = 2.08596$		
Level		Least Sq Mean	Level		Least Sq Mean
CI,HMA	A	5313.5630	ESO,WMA	A	26.803580
RP,HMA	A B	5060.4235	EMS,HMA	A B	26.015926
Control,HMA	B C	4718.7852	RP,WMA	B C	25.764074
ESO,HMA	C D	4631.0284	RP,HMA	B C	25.718765
EMS,HMA	C D	4616.7790	EMS,WMA	B C	25.602840
RP,WMA	C D	4566.4481	CI,WMA	B C	25.586543
ESO,WMA	D E	4290.9025	Control,WMA	B C	25.485062
CI,WMA	D E	4284.1383	Control,HMA	C D	25.133333
Control,WMA	E	4146.2198	CI,HMA	C D	24.956667
EMS,WMA	E	4102.4000	ESO,HMA	D	24.368395
Levels not connected by same letter are significantly different.			Levels not connected by same letter are significantly different.		
(a)			(b)		

Fig. 8. Student's  $t$ -test least square means difference for interaction A\*B (a)  $E^*$  (MPa), and (b)  $\delta$  (°).

## 5. Conclusions & recommendations

Through modifications of previously made  $E^*$  and  $\delta$  models, it is shown that the developed PN model works as well or better than the sigmoidal, Yang and You, and Booi and Thoone models in the determination of  $E^*$  and  $\delta$  master curves. The PN model demonstrated that it is possible to not lose precision and accuracy in the determination of  $E^*$  master curves while co-determining  $\delta$  master curves. Based upon the master curve results it was observed that some, but not all of the corn and soybean based materials may be affecting the viscous behavior at intermediate and high test temperatures. This is based on visual evidence

showing a clear trend between using WMA and HMA compaction temperatures as the corn and soybean based material appear to make the dynamic modulus higher than the control HMA at high test temperatures when used in producing HMA vs. making WMA. There is not enough evidence to make conclusions that align with conclusions made in previous research using the same materials in HWTB testing, that WMA produced with the same corn and soybean based materials perform better against stripping than a WMA control. Specimens in the previous study made with additives were only produced at WMA compaction temperatures. Based upon this likelihood of improved moisture susceptibility Hamburg Wheel



Tracking Device testing should be done in the future on these mix combinations.

### Disclosure statement

No potential conflict of interest was reported by the authors.

### References

- [1] J. D'Angelo, E. Harm, J. Bartoszek, G. Baumgardner, M. Corrigan, J. Cowser, T. Harman, M. Jamshidi, W. Jones, D. Newcomb, B. Prowell, R. Sines, B. Yeaton., Warm-mix asphalt: European practice, Publication FHWA-PL-08-007, FHWA, U.S. Dept. of Transportation, Washington, DC, 2008.
- [2] D. Newcomb, An introduction to warm mix asphalt, National Asphalt Pavement Association (2007).
- [3] M. Hassan Life-cycle assessment of warm-mix asphalt: An environmental and economic perspective, Transportation Research Board 88th Annual Meeting, Washington, DC, 2009.
- [4] Ó. Kristjánssdóttir, S.T. Muench, L. Michael, G. Burke, Assessing potential for warm-mix asphalt technology adoption, *Transp. Res. Rec.* 2040 (2007) 91–99.
- [5] K. Jenkins, J. De Groot, M. van de Ven, A. Molenaar, Half-warm foamed bitumen treatment, a new process, 7th Conference on asphalt pavements for Southern Africa (CAPSA 99), 1999.
- [6] Ó. Kristjánssdóttir, *Warm-mix Asphalt for Cold Weather Paving*, Univ. of Washington, Seattle, WA, 2006.
- [7] O. Larsen, Ø. Moen, C. Robertus, B. Koenders, WAM Foam asphalt production at lower operating temperatures as an environmental friendly alternative to HMA, 3rd Eurasphalt & Eurobitume Congress, Foundation Eurasphalt, Breukelen, Netherlands., 2004.
- [8] R. Anderson, G. Baumgardner, R. May, G. Reinke, Engineering Properties, Emissions, and Field Performance of Warm Mix Asphalt Technologies. NCHRP 9-47, Interim Report, National Cooperation Highway Research Program, Washington, DC (2008).
- [9] B. Koenders, D. Stoker, C. Robertus, O. Larsen, J. Johansen, WAM-foam, asphalt production at lower operating temperatures, Ninth International Conference on Asphalt Pavements, 2002.
- [10] B. Middleton, R. Forfyflow, Evaluation of warm-mix asphalt produced with the double barrel green process, *Transp. Res. Rec.* 2126 (2009) 19–26.
- [11] Z. Hossain, M. Zaman, E.A. O'Rear, D.-H. Chen, Effectiveness of Advera® in Warm Mix Asphalt, GeoHunan International Conference 2011, 2011.
- [12] G.C. Hurley, B.D. Prowell, Evaluation of Aspha-Min zeolite for use in warm mix asphalt, NCAT report 05-04, 2005.
- [13] J. Button, C. Estakhri, A. Wimsatt, A synthesis of warm mix asphalt. Rep. No, FHWA/TX-07/0-5597-1. Texas Transportation Institute, Texas A&M University System, 2007.
- [14] M. Corrigan, Warm mix asphalt technologies and research, *Federal Highway Admin. Off. Pavement Technol.* 3 (10) (2006) 26–28.
- [15] G.C. Hurley, B.D. Prowell, Evaluation of Sasobit for use in warm mix asphalt, NCAT report 05-06, 2005.
- [16] G.C. Hurley, B.D. Prowell, Evaluation of Evotherm for use in warm mix asphalt, NCAT Rep. 06-02, 2006.
- [17] T.A. Werpy, J.E. Holladay, J.F. White, Top Value Added Chemicals From Biomass: I. Results of Screening for Potential Candidates from Sugars and Synthesis Gas, 2004, p. Medium: ED; Size: PDFN.
- [18] A. Buss, J. Podolsky, R.C. Williams, E. Cochran, Investigation of isosorbide distillation bottoms as a bio-based warm-mix additive, *J. Mater. Civil Eng.* 28 (3) (2016) 04015153.
- [19] J.H. Podolsky, A. Buss, R.C. Williams, E.W. Cochran, The rutting and stripping resistance of warm and hot mix asphalt using bio-additives, *Constr. Build. Mater.* 112 (2016) 128–139.
- [20] S. Diefenderfer, A. Hearon, Laboratory evaluation of a warm asphalt technology for use in Virginia, (No. FHWA/VTRC 09-R11), 2008.
- [21] R. Ghabchi, D. Singh, M. Zaman, Laboratory evaluation of stiffness, low-temperature cracking, rutting, moisture damage, and fatigue performance of WMA mixes, *Road Mater. Pavement Des.* 16 (2) (2015) 334–357.
- [22] B. Prowell, G. Hurley, E. Crews, Field performance of warm-mix asphalt at national center for asphalt technology test track, *Transp. Res. Rec.* 1998 (1) (2007) 96–102.
- [23] B.D. Prowell, G.C. Hurley, B. Frank, Warm-mix Asphalt: Best Practices, National Asphalt Pavement Association Lanham, Maryland, USA, 2011.
- [24] F. Xiao, S. Amirkhanian, B. Putman, Evaluation of rutting resistance in warm-mix asphalts containing moist aggregate, *Transp. Res. Rec.* 2180 (2010) 75–84.
- [25] H. Zelelew, C. Paugh, M.R. Corrigan, Warm-Mix Asphalt Laboratory Permanent Deformation Performance in State of Pennsylvania: Case Study, Transportation Research Board 90th Annual Meeting, 2011.
- [26] J.H. Podolsky, Investigation of Bio-derived Material and Chemical Technologies as Sustainable Warm Mix Asphalt Additives, Civil, Construction and Environmental Engineering, Iowa State University, Ames, 2014, p. 209.
- [27] A. Buss, Y. Kuang, R.C. Williams, J. Bausano, A. Cascione, S.A. Schram, Influence of Warm Mix Asphalt Additive and Dosage Rate on Construction and Performance of Bituminous Pavements, Transportation Research Board 93rd Annual Meeting, 2014.
- [28] E.R. Brown, P.S. Kandhal, F.L. Roberts, Y.R. Kim, D.-Y. Lee, T.W. Kennedy, National Asphalt Pavement Association., NAPA Research and Education Foundation., National Center for Asphalt Technology (U.S.), Hot mix asphalt materials, mixture design, and construction, 3rd ed., NAPA Research and Education Foundation, Lanham, Md., 2009.
- [29] D.W. Christensen, D.A. Anderson, Interpretation of dynamic mechanical test data for paving grade asphalt cements (with discussion), *J. Assoc. Asphalt Paving Technol.* 61 (1992).
- [30] X.J. Li, R.C. Williams, A practical dynamic modulus testing protocol, *J. Test. Eval.* 40 (1) (2012) 100–106.
- [31] T. Pellinen, M. Witczak, Stress dependent master curve construction for dynamic (complex) modulus (with discussion), *J. Assoc. Asphalt Paving Technol.* 71 (2002) 281–309.
- [32] H.C. Booij, G.P.J.M. Thoone, Generalization of Kramers–Kronig transforms and some approximations of relations between viscoelastic quantities, *Rheol. Acta* 21 (1) (1982) 15–24.
- [33] X. Yang, Z. You, New predictive equations for dynamic modulus and phase angle using a nonlinear least-squares regression model, *J. Mater. Civil Eng.* 27 (3) (2015).
- [34] Z. You, S.W. Goh, J. Dong, Predictive models for dynamic modulus using weighted least square nonlinear multiple regression model, *Can. J. Civil Eng.* 39 (5) (2012) 589–597.
- [35] T.K. Pellinen, M.W. Witczak, R.F. Bonaquist, Asphalt Mix Master Curve Construction Using Sigmoidal Fitting Function with Non-Linear Least Squares Optimization, 15th Engineering Mechanics Division Conference, ASCE, 2003, pp. 83–101.
- [36] A.S.M.A. Rahman, R.A. Tarefder, Dynamic modulus and phase angle of warm-mix versus hot-mix asphalt concrete, *Constr. Build. Mater.* 126 (2016) 434–441.